

Synthesis and Catalytic Property of PtSn/C Toward the Ethanol Oxidation Reaction

Bing-Jian Su¹, Kuan-Wen Wang², Chung-Jen Tseng^{1,*}, Chih-Hao Wang¹, Yu-Jui Hsueh¹

¹ Department of Mechanical Engineering, National Central University, Chungli 32001 Taiwan

² Institute of Materials Science and Engineering, National Central University, Chungli 32001 Taiwan

*E-mail: cjtseng@ncu.edu.tw

Received: 1 May 2012 / Accepted: 19 May 2012 / Published: 1 June 2012

Nanosized PtSn/C catalysts with good dispersion and high catalytic activity toward the ethanol oxidation reaction (EOR) were prepared successfully by an alcohol reduction process. The pH value of the refluxing solution during the preparation was controlled at 9 or 12 to enhance the EOR activity of the prepared catalysts. The compositions, phase structures, morphological properties, EOR activity and durability of the electrocatalysts were characterized by energy dispersive spectrometry, X-ray diffraction, high-resolution transmission electron microscopy, cyclic voltammetry, and a long term test, respectively. It was found that for the PtSn/C catalysts the particle size, EOR activity and durability are affected by the pH value during the preparation. Because of the formation of SnO₂ phases, the PtSn/C prepared at pH 12 (Sn12) has a smaller particle size than that prepared at pH 9 (Sn9). Both the Sn9 and Sn12 samples show a lower onset potential and a higher Pt mass current density in the low potential region for the EOR compared with commercial Pt/C. The Pt mass current density at E = 0.6 V (*I*₀₆) is 33.1, 16.5, and 12.4 mA/mg for Sn12, Sn9, and Pt/C, respectively. For the chronoamperometry test, the activity of the Sn12 catalysts is much higher than that of Pt/C after 3600 s suggesting that the Sn12 catalysts have better stability and poisoning tolerance.

Keywords: PtSn/C; alcohol reduction process; ethanol oxidation reaction (EOR); pH value; stability

1. INTRODUCTION

In recent years, massive utilization of natural resources such as fossil fuels has caused significant environmental pollution. The greenhouse effect, acid rain, and the destruction of the ozonosphere are becoming more serious [1–3]. Finding renewable and clean energy is becoming urgent to replace traditional power generation methods. With this in mind, hydrogen energy and fuel cells are promising candidates [5–8]. Fuel cells convert chemical energy directly into electrical energy and have high efficiency, high power density, and low or zero emission of pollutants [9–12]. Additionally, fuel cells can be used in transportation vehicles as well as other automotive, portable,

and stationary applications. Polymer electrolyte membrane fuel cells (PEMFCs) and direct alcohol fuel cells (DAFCs) have been studied extensively because they can operate at low temperatures quietly with fast start-up and shutdown [13-15]. DAFCs are especially suitable for small electronic devices such as cellular phones and laptops [16]. However, the production and storage of hydrogen and/or the use of fuel reformers limits the application of PEMFCs [1]. Contrary to gaseous hydrogen carriers, liquid hydrogen carriers such as methanol and ethanol have the advantage of high theoretical volumetric energy density and ease of storage and transportation. Therefore, DAFCs have been extensively studied as promising devices and alternative power sources [17-19].

In various types of DAFCs, direct methanol fuel cells (DMFCs) and direct ethanol fuel cells (DEFCs) are widely proposed for use in mobile applications. Currently, the DMFC is the simplest DAFC and methanol is one of the most electroactive fuels [20-22]. However, since methanol is volatile, relatively toxic, and easily miscible with water it is not considered a friendly fuel. On the other hand, ethanol is a good substitute because it is safer, has a higher theoretical energy density, and is less toxic than methanol [23]. Moreover, as a green fuel this alcohol can be obtained from biomass and can be easily produced by fermentation [24]. Therefore, the study of DEFCs has attracted much attention.

In terms of DEFCs, it is a real challenge to increase the electroactivity of the ethanol oxidation reaction (EOR) in the anode because the EOR is a complicated multistep reaction. The C–C bond needs to be broken to completely oxidize ethanol to CO₂ [25]; otherwise, a number of adsorbed intermediates and byproducts from an incomplete EOR will be obtained [26]. Therefore, overcoming the sluggish kinetics of the EOR is required. Although carbon supported Pt (Pt/C) electrocatalysts are known to be the best material for alcohol oxidation, Pt can be easily poisoned by strongly adsorbed species such as CO [17, 23, 24]. By adding second or third metals to Pt to form alloy structures the EOR activity can be enhanced [17]. Many different Pt-based anode catalysts such as PtRu [27], PtSn [28, 29], and PtAu [30] have been investigated and reported to increase the EOR activity. Among these binary and ternary alloy catalysts, PtSn catalysts are state of the art catalysts for the EOR. Moreover, based on the bifunctional mechanism and the ligand effect [1] some researchers have also shown that SnO₂ can provide O-species for the oxidation of the CO that is produced on the Pt active sites during the dissociative adsorption of ethanol [31, 32]. The role of SnO₂ during the EOR activity of the PtSn catalysts has been proposed [33]. The authors showed that SnO₂ can increase the Pt surface area or help remove the adsorbed intermediates.

Although there are a few studies on PtSn/C catalysts, the effects of the pH value of the solution during the preparation process on the electroactivity of the catalyst have not been addressed. We will investigate the effects of the pH value in the work. The PtSn/C catalysts were prepared by alcohol reduction, which allows for the preparation of small and well-dispersed metal/alloy nanoparticles on the support. Ethylene glycol (EG) serves as a reducing agent and a solvent during the preparation. The pH value of the solution that consists of metal salts and EG was controlled at 9 or 12 to study the effect of SnO₂ on EOR performance. The structures, morphologies, and electroactivities of the obtained PtSn/C catalysts were analyzed by X-ray diffraction (XRD), high resolution transmission electron microscopy (HRTEM), energy dispersive spectrometry (EDS), and cyclic voltammetry (CV), respectively.

2. EXPERIMENT

2.1. Preparation of catalysts

PtSn/C catalysts with a 20 wt% metal loading were prepared by alcohol reduction. The precursors chloroplatinic acid ($\text{H}_2\text{PtCl}_6 \cdot 6\text{H}_2\text{O}$, Aldrich) and tin chloride ($\text{SnCl}_2 \cdot \text{H}_2\text{O}$, Alfa Aesar) were dissolved in 100 ml EG (Merck) and the pH of the solution was controlled at 9 or 12. The carbon support (Vulcan Xc72R, Vulcan) was then added and the mixture was refluxed at 160 °C for 3 h under N_2 . Finally, the powders were filtered, washed, and dried at 50 °C for 24 h. The samples reduced at pH 9 and 12 are designated Sn9 and Sn12, respectively.

2.2. Characterization of the catalysts

The Pt to Sn atomic ratios were examined by EDS analysis using scanning electron microscopy (SEM, JEOL JSM-7401F) with a 15 keV electron beam. The alloy structures of the catalysts were determined by XRD using a Siemens D-5000 with a Cu $K\alpha$ radiation source. The morphology of the home-made catalyst was analyzed by HRTEM (JEOL JEM-2100) operated at 300 keV.

Electrochemical measurements of the electrocatalysts were performed in a standard three-compartment electrochemical cell with reference and counter electrodes in separate compartments to the working electrode. The alloy catalysts (5 mg, including the home-made catalysts and the commercial 20 wt% Pt/C catalyst from E-Tek) were dispersed in an ultrasonic solution of 1 ml deionized water and 5 μl 5% Nafion® solution for 40 min, and we obtained a well-dispersed catalyst ink. The catalyst ink (10 μl) was transferred to a glassy carbon disk (0.196 cm^2) of the working electrode by a micropipette. The final Pt loading on each electrode was ca. 9.5 and 7.1 μg for the commercial sample and the bimetallic PtSn/C, respectively. Ag/AgCl electrode and Pt wire served as the reference and counter electrodes, respectively. Cyclic potentials were swept between -0.2 and 0.8 V (vs. Ag/AgCl) at a rate of 20 mV/s at room temperature. The electrolyte containing 0.5 mol/L H_2SO_4 + 1 mol/L $\text{C}_2\text{H}_5\text{OH}$ was pre-purged with N_2 for 30 min before CV characterization. All the reported CV characterizations were recorded in the 16th cycle. The chronoamperometry test of the catalysts was measured at a potential of 0.36 V (vs. SCE) for 1 h. The current density toward the EOR was normalized to the weight of Pt in the catalysts. All the potentials quoted are relative to the normal hydrogen electrode (NHE).

3. RESULTS AND DISCUSSION

3.1. EDS analysis of the PtSn/C catalysts

The atomic ratios of Pt:Sn for the two PtSn/C catalysts deposited at different pH values were determined by EDS and are listed in Table 1. The Pt:Sn ratio was found to be about 63:37, and this deviates from the nominal atomic ratio of 75:25 suggesting that some Pt may be lost during the

preparation process. On the other hand, the atomic ratio of Pt:Sn was not affected significantly by the pH value of the reducing solvent.

Table 1. EDS, XRD, TEM, and electrochemical results of commercial Pt/C and home-made PtSn catalysts.

Sample	EDS (at %)		Size (nm)		XRD phase	I06 (mA/mgPt)
	Pt	Sn	XRD ^a	TEM ^b		
Sn9	62	38	5.9	4.1 ± 0.7	C, Pt, Sn	16.5
Sn12	63	37	5.6	3.8 ± 3.6	C, Pt, SnO ₂	33.1
Pt/C						12.4

a Calculated using the Scherrer formula.
b Obtained from TEM measurement.

3.2. XRD characterization of the PtSn/C catalysts

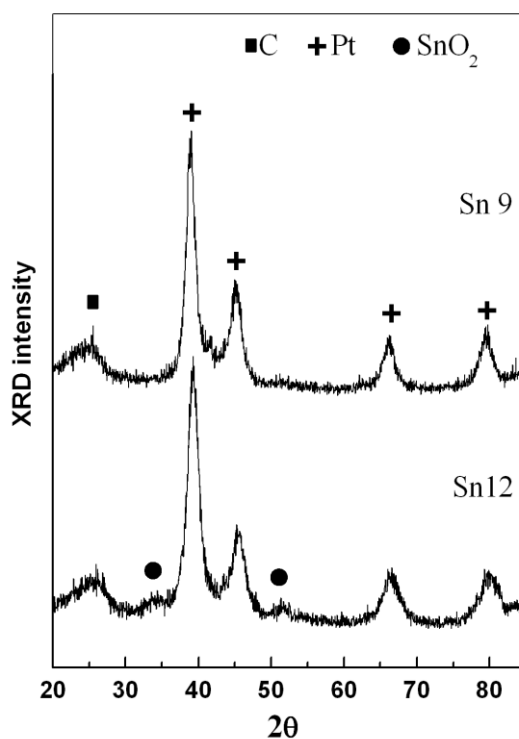


Figure 1. XRD patterns of the PtSn/C catalysts prepared by different methods.

Figure 1 shows the phase structures of the PtSn/C catalysts that were prepared at different pH values and the average particle sizes for the PtSn/C catalysts calculated from the (111) reflections are listed in the third column of Table 1. The first broad diffraction peak located at $2\theta = 25^\circ$ is assigned to the (002) reflection of the carbon support. For metallic Pt (JCPDS 04-0802) the (111), (200), (220), and (311) peaks are present at $2\theta = 39.8^\circ$, 46.2° , 67.5° , and 81.2° , respectively. Therefore, the

diffraction peaks observed at $2\theta = 39.3^\circ$, 45.2° , 66.6° , and 79.3° are attributed to the (111), (200), (220), and (311) diffractions of Pt-based alloys, respectively. We found that the addition of Sn causes the reflection peak to shift negatively. In addition, the two peaks at $2\theta = 33.8^\circ$ and 51.3° are assigned to the SnO_2 phase (JCPDS 41-1445) for the Sn12 sample. Lim et al. [9] prepared various PtSn/C catalysts by borohydride reduction and they added 5 mol/L of NaOH solution slowly to the precursor solvent until the pH value reached 11. SnO_2 diffraction peaks were also found in the alloy catalysts. Therefore, when reduced at high pH value, the C, Pt-based alloy, and SnO_2 phases coexist in the PtSn/C catalysts indicating that the pH value of the reflux process is an important factor for the alcohol reduction method. Moreover, the crystalline size of Sn9 and Sn12 based on the XRD pattern was found to be about 5.9 and 5.6 nm, respectively. It seems that SnO_2 may increase the dispersion and decrease the size of the alloy nanoparticles on C support so that the catalysts prepared at pH 12 have a smaller size than those prepared at pH 9.

3.3. HRTEM images of the PtSn/C catalysts

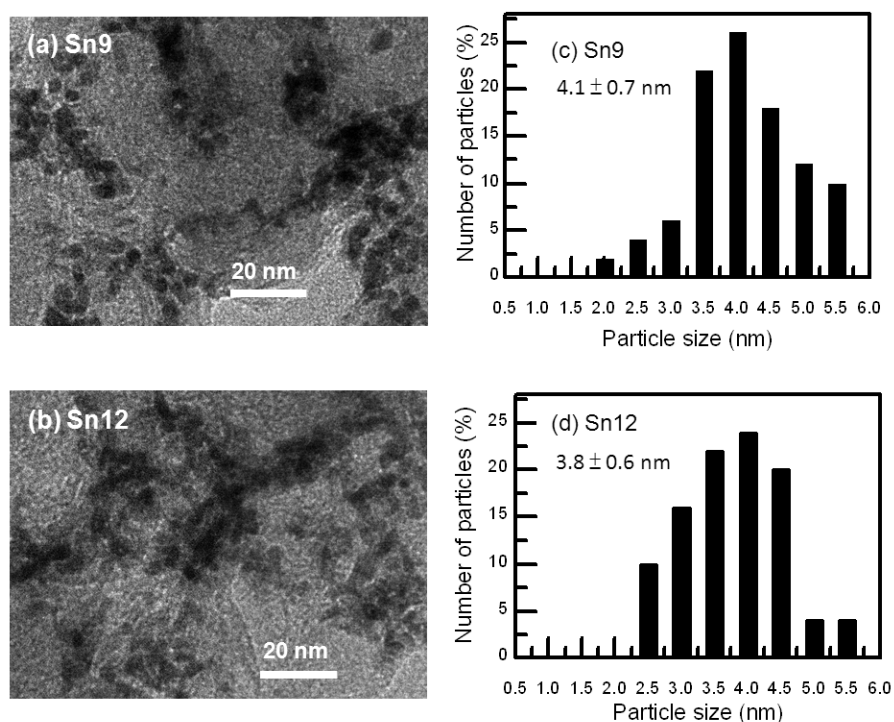


Figure 2. HRTEM micrographs and particle size distributions of the PtSn/C catalysts prepared at different pH values. (a) and (c) Sn9; (b) and (d) Sn12.

HRTEM images of the two PtSn/C catalysts are shown in Figure 2, and the averaged particle sizes are presented also in Table 1 for comparison. For the home-made PtSn/C catalysts, the nanoparticles are well dispersed on the C support. The particle sizes of Sn9 and Sn12 are about 4.1 and 3.8 nm, respectively. This is fairly consistent with the XRD results. Therefore, EG is generally a reducing agent and a solvent that can be used to prepare small nanoparticles that are highly dispersed.

The particle size distributions for samples Sn9 and Sn12 are shown in Figure 2(c) and (d), and the particle size distribution of Sn12 is narrower than that of Sn9, which confirms that SnO₂ can enhance the dispersion and decrease the size of the PtSn/C particles.

3.4. EOR of the PtSn/C and Pt/C catalysts

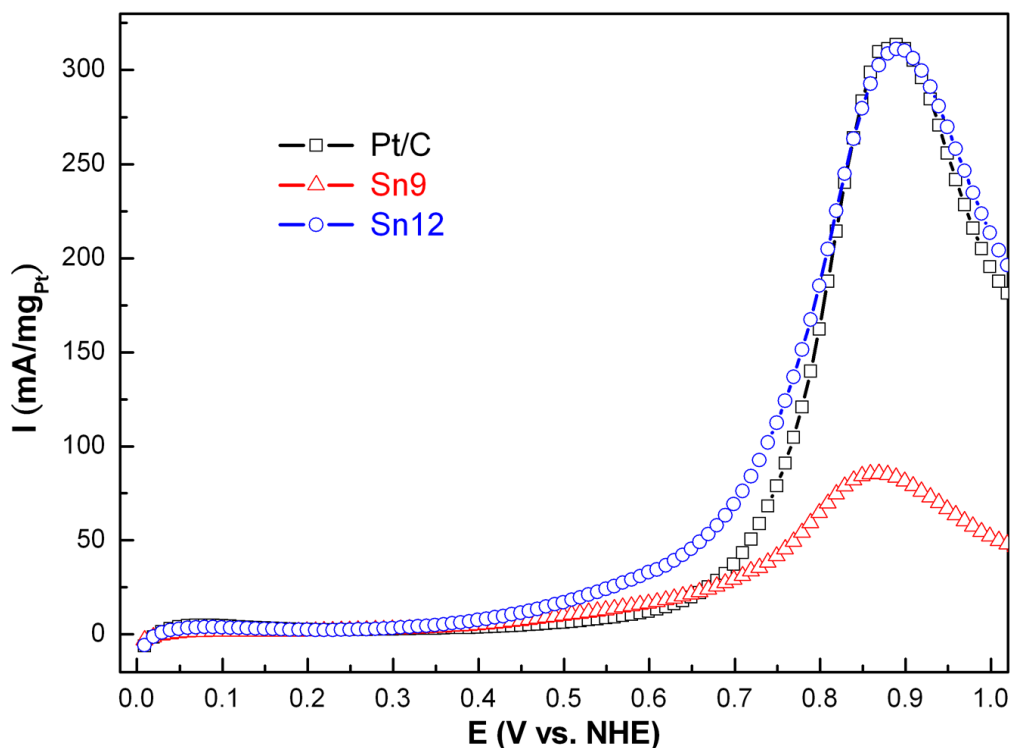
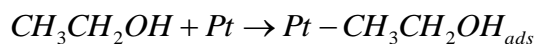


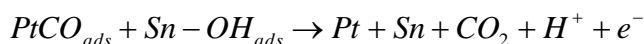
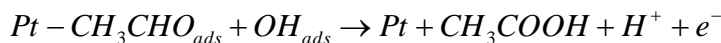
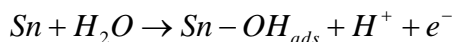
Figure 3. The forward CV scans of the PtSn/C and the Pt/C catalysts for the EOR in 0.5 mol/L H₂SO₄ and 1 mol/L C₂H₅OH.

Figure 3 shows forward CV scans for the EOR over various catalysts. Sn9 and Sn12 have lower onset potentials than commercial Pt/C. In the low potential region ($E < 0.65$ V), the home-made PtSn/C catalysts, especially Sn12, show higher activity toward the EOR than Pt/C. It has been reported that Pt₃Sn/C shows a lower onset potential than commercial Pt/C [3, 4]. The Pt₃Sn/C catalyst was reported to show an appropriate expansion of lattice parameters and that Sn oxide is present. The proper expansion of lattice parameters in the PtSn alloy improved adsorption and dissociation during the oxidation reaction. However, according to Figure 1, the enhanced EOR performance of the Sn12 sample in this work is due to the SnO₂ phase instead of the Pt₃Sn phase. Liu et al. [34] pointed out that the SnO₂ on the catalyst surface may enhance the oxidation of adsorbed CO to CO₂ completely and promote electrochemical activity. The Pt mass current density at $E = 0.6$ V ($I_{0.6}$) is 16.5, 33.1, and 12.4 mA/mg for Sn9, Sn12, and Pt/C, respectively, as listed in Table 1.

Li et al. [24] determined the rate determining step (RDS) of PtSn/C in different potential regions. The dissociative adsorption of ethanol on the Pt surface is the main step in the lower potential region:



However, for higher potential regions the RDS is the activation of H_2O oxidation to OH^- . The mechanism at higher potential region can be described by the following equations:



Therefore, SnO_2 can improve Pt for the quick dissociation of ethanol in higher potential region. However, there may be too many oxides on the alloy surface to block the active sites on the Pt nanoparticles, which would deteriorate the electrochemical activity [35].

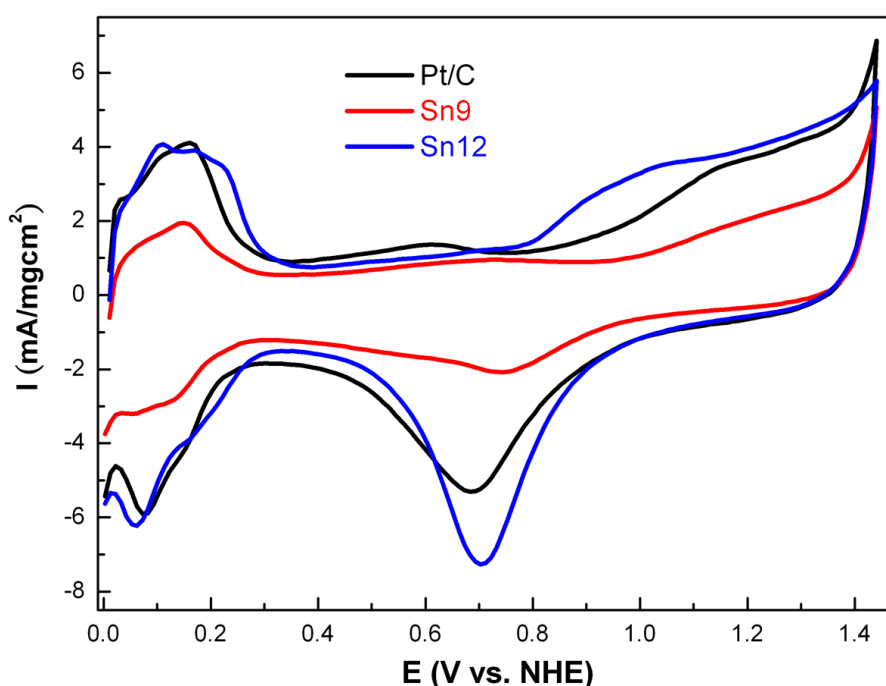


Figure 4. CVs of the PtSn/C and the Pt/C catalysts in a 0.5 M H_2SO_4 with a scan rate of 20 mVs^{-1} .

It has been found that the catalytic activity is influenced by the preparation method of the catalysts. Moreover, SnO_2 can increase the Pt surface area or help in the removal of adsorbed intermediates by a bi-functional mechanism [9], which plays an important role in enhancing the EOR activity. The CVs of the Pt/C and the PtSn/C catalysts as measured in 0.5 mol/L H_2SO_4 are shown in Figure 4. A H-adsorption peak in the potential region from 0 to 0.3 V (vs. NHE) is clearly present. The electrochemical active surface areas are 57, 34, and $68 \text{ m}^2/\text{g}$ for Pt/C, Sn9, and Sn12, respectively. Therefore, SnO_2 can increase the surface area of Pt. Sn12 containing a SnO_2 phase in the alloy catalysts shows higher EOR activity than Pt/C.

3.5. Chronoamperometry of the PtSn/C and Pt/C catalysts

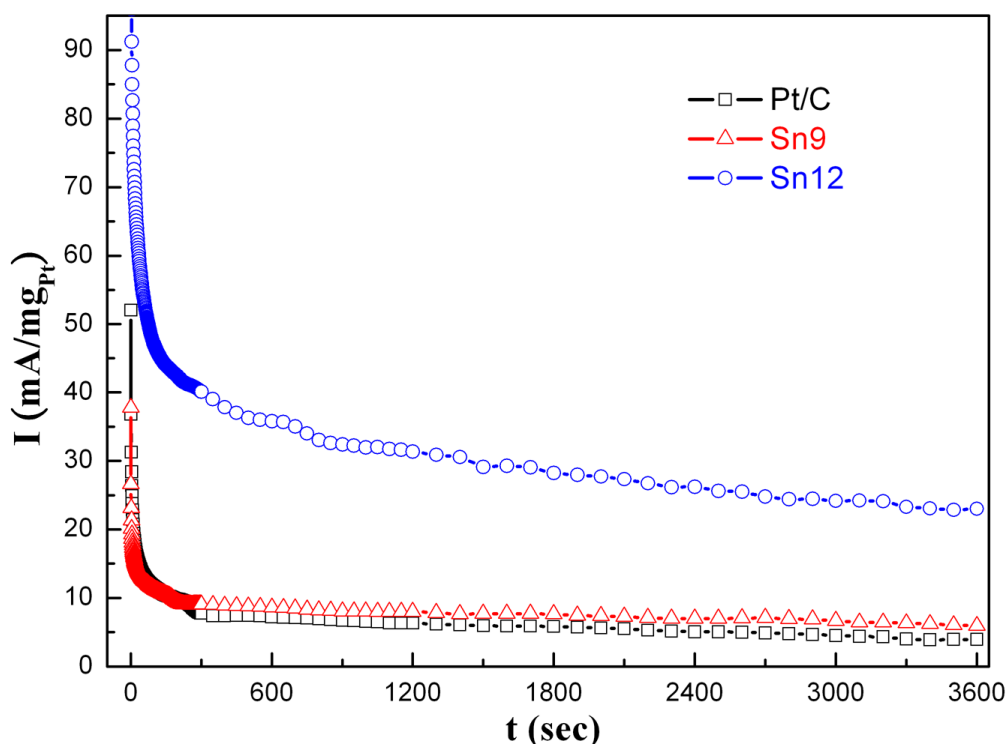


Figure 5. Chronoamperometry test of the PtSn/C and Pt/C catalysts at 0.6 V (vs. NHE) over 1 h in 0.5 mol/L H_2SO_4 and 1 mol/L $\text{C}_2\text{H}_5\text{OH}$.

It is known that intermediates such as CO_{ads} and acetic acid etc. may be produced when ethanol is oxidized to CO_2 . The surface and active sites will be largely occupied by these species, which poisons the catalysts and the kinetics of the EOR is quickly reduced.

Table 2. The electrocatalytic properties of commercial Pt/C and home-made PtSn catalysts

Sample	onset potential (V)	electric quantity of EORa	EASAs (m^2g^{-1})	electric quantity of CC methodb
Pt/C	0.45	76.7	57	22027
Sn9	0.38	19.4	34	27887
Sn12	0.30	89.3	68	108815

a Calculated by integrating the EOR peak.
b Calculated by integrating the areas under the CA curves.

Chronoamperometry tests for the EOR at 0.6 V (vs. NHE) were carried out over 1 h and the results are shown in Figure 5. Initially, the catalysts are poisoned by CO_{ads} during the EOR and the current density drops quickly before becoming stable. The EOR current density of Sn9 and Sn12 is higher than that of Pt/C, which is in good agreement with the CV results shown in Figure 3. Moreover, the current density of Sn12 is still 5.7 times higher than that of Pt/C after 1 h suggesting that the Sn12

catalysts have better stability and poisoning tolerance. Iwasita and Pastor [26] have also reported that SnO₂ can modify the electronic structure of Pt and weaken the O-O double bond. As discussed above, SnO₂ plays an important role in enhancing EOR activity and it allows ethanol to oxidize completely.

4. CONCLUSIONS

Nanosized PtSn/C with high dispersion has been prepared by alcohol reduction for use in the EOR. The pH value of the refluxing solution was controlled at 9 or 12 during the preparation to optimize the EOR activity of the catalysts. Based on the XRD and HRTEM measurements, the sample prepared at pH 12 has a smaller particle size and better dispersion than that prepared at pH 9 because of the formation of SnO₂ phases in PtSn/C catalysts. Furthermore, the Sn9 and Sn12 samples showed a higher Pt mass current density and a more negative onset potential for the EOR than commercial Pt/C. The chronoamperometry test confirmed that Pt9 and Pt12 have about 1.3 and 5.7 times higher mass current density at E = 0.6 V than commercial Pt/C, respectively. As a result, the Sn12 catalysts have better stability and poisoning tolerance suggesting that SnO₂ plays an important role in enhancing the EOR activity and allowing ethanol oxidation to complete.

ACKNOWLEDGEMENT

This work was supported by the National Science Council of Taiwan under Contract Nos. NSC-100-2622-E-008-002-CC2, NSC 101-3113-P-008-006, NSC 100-2923-E-239 -001 -MY3.

References

1. F. Vigier, C. Coutanceau, F. Hahn, E. M. Belgsir and C. Lamy, *J. Electroanal Chem.*, 563 (2004) 81.
2. M. Momirlan and T.N. Veziroglu, *Renew Sust Energ Rev*, 6 (2002) 141.
3. K. W. Wang, S. Y. Huang and C. T. Yeh, *J. Phys. Chem. C*, 111 (2007) 5096.
4. S. Dunn, *Int J Hydrogen Energy*, (2001) 235.
5. C.L. Tseng, C.J. Tseng and J.C. Chen, *In. J Hydrogen Energ*, 35 (2010) 2781.
6. C. H. Wang, K. W. Cheng and C. J. Tseng, *Sol Energ Mat Sol C*, 95 (2011) 453.
7. C.J. Tseng and C.L. Tseng, *Int J Hydrogen Energ*, 36 (2011) 6510.
8. S. K. Lo, C. J. Tseng, L. D. Tsai and J.N. Lin, *J Chin Inst Eng*, 34 (2011) 39.
9. D. H. Lim, D. H. Choi, W. D. Lee and H. I. Lee, *Appl. Catal. B*, 89 (2009) 484.
10. C. J. Tseng, S. T. Lo, S. C. Lo and P. P. Chu, *Mater. Chem. Phys.*, 100 (2006) 385.
11. Y. C. Wei, C. W. Liu and K. W. Wang, *ChemPhysChem.*, 10 (2009) 1230.
12. L. Carrette, K. A. Friedrich and U. Stimming, *ChemPhysChem.*, 1 (2000) 162.
13. Y. C. Wei, C. W. Liu, Y. W. Chang and K. W. Wang, *Int. J Hydrogen Energy*, 34 (2010) 1383.
14. H. Li, D. Kang, H. Wang and R. Wang, *Int. J. Electrochem. Sci.*, 6 (2011) 1058.
15. C.J. Tseng and S.K. Lo, *Energ Convers Manage*, 51 (2010) 677.
16. L. Zhang, K. Lee and J. Zhang, *Electrochim. Acta*, 52 (2007) 3088.
17. W. Zhou, Z. Zhou, S. Song, W. Li, G. Sun, P. Tsiakaras and Q. Xin, *Appl Catal B: Environ*, 46 (2003) 273.
18. F. Ren, F. Jiang, Y. Du, P. Yang, C. Wang and J. Xu, *Int. J. Electrochem. Sci.*, 6 (2011) 5701.
19. Y. Guo, Y. Zheng and M. Huang, *Electrochim. Acta*, 53 (2008) 3102.

20. T. Frelink, W. Visscher and J. A. R. Van Veen, *Langmuir*, 12 (1996) 3702.
21. S. Wasmus and A. Kuver, *J. Electroanal. Chem.*, 461 (1999) 14.
22. H. D. Herrera-Méndez, P. Roquero, M. A. Smit and L. C. Ordóñez, *Int. J. Electrochem. Sci.*, 6 (2011) 4454.
23. C. Lamy, S. Rousseau, E. M. Belgsir, C. Coutanceau and J. M. Leger, *Electrochim. Acta*, 49 (2004) 3901.
24. H. Li, G. Sun, L. Cao, L. Jiang and Q. Xin, *Electrochim. Acta*, 52 (2007) 6622.
25. H. Honala and Y. Matsumura, *J. Electroanal. Chem.*, 520 (2002) 101.
26. T. Iwasita and E. Pastor, *Electrochim. Acta*, 39 (1994) 531.
27. E.V. Spinace, A.O. Neto and M. Linardi, *J. Power Sources*, 129 (2004) 121.
28. R. M. Piasentin, E. V. Spinacé, M. M. Tusi and A. O. Neto, *Int. J. Electrochem. Sci.*, 6 (2011) 2255.
29. A. T. Aoul, F. Saidani, D. Rochefort and M. Mohamedi, *Int. J. Electrochem. Sci.*, 6 (2011) 6385.
30. G.Tremiliosi-Filho, E. R. Gonzalez and A. J. Motheo, *J. Electroanal. Chem.*, 444 (1998) 31.
31. J. C. M. Silvea, R. F. B. Souza, L. S. Parreira, E. Teixeira Neto, M. L. Calegari and M. C. Santos, *Appl. Catal. B*, 99 (2010) 265.
32. Y. W. Chang, C. W. Liu, Y. C. Wei and K. W. Wang, *Electrochem. Commun.*, 11 (2009) 2161.
33. E. Antolini and E. R. Gonzalez, *Catalysis Today*, 160 (2011) 28.
34. Z. Liu, X. Y. Ling, X. Su and Y. Lee, *J Phys Chem B*, 108 (2004) 8234.
35. C. W. Liu, Y. W. Chang, Y. C. Wei and K. W. Wang, *Electrochim Acta*, 56 (2011) 2574.